J Ginseng Res 43 (2019) 10–19

Contents lists available at ScienceDirect

Journal of Ginseng Research

journal homepage: http://www.ginsengres.org

Research article

Ginsenoside Rk1 ameliorates paracetamol-induced hepatotoxicity in mice through inhibition of inflammation, oxidative stress, nitrative stress and apoptosis

Jun-Nan Hu [1], Xing-Yue Xu [1], Wei Li [1,2,5,*], Yi-Ming Wang [3], Ying Liu [1,4], Zi Wang [1,5], Ying-Ping Wang [2,5]

[1] College of Chinese Medicinal Materials, Jilin Agricultural University, Changchun, China
[2] Institute of Special Wild Economic Animals and Plant, CAAS, Changchun, China
[3] College of Animal Science and Technology, Jilin Agricultural University, Changchun, China
[4] Department of Oriental Medicinal Biotechnology, College of Life Science, Kyung Hee University, Republic of Korea
[5] National & Local Joint Engineering Research Center for Ginseng Breeding and Development, Changchun, China

ARTICLE INFO

Article history:
Received 9 February 2017
Received in Revised form
21 June 2017
Accepted 20 July 2017
Available online 25 July 2017

Keywords:
anti-inflammation
anti-apoptosis
APAP-induced hepatotoxicity
ginsenoside Rk1
oxidative stress

ABSTRACT

Background: Frequent overdose of paracetamol (APAP) has become the major cause of acute liver injury. The present study was designed to evaluate the potential protective effects of ginsenoside Rk1 on APAP-induced hepatotoxicity and investigate the underlying mechanisms for the first time.
Methods: Mice were treated with Rk1 (10 mg/kg or 20 mg/kg) by oral gavage once per d for 7 d. On the 7th d, all mice treated with 250 mg/kg APAP exhibited severe liver injury after 24 h, and hepatotoxicity was assessed.
Results: Our results showed that pretreatment with Rk1 significantly decreased the levels of serum alanine aminotransferase, aspartate aminotransferase, tumor necrosis factor, and interleukin-1β compared with the APAP group. Meanwhile, hepatic antioxidants, including superoxide dismutase and glutathione, were elevated compared with the APAP group. In contrast, a significant decrease in levels of the lipid peroxidation product malondialdehyde was observed in the ginsenoside Rk1-treated group compared with the APAP group. These effects were associated with a significant increase of cytochrome P450 E1 and 4-hydroxynonenal levels in liver tissues. Moreover, ginsenoside Rk1 supplementation suppressed activation of apoptotic pathways by increasing Bcl-2 and decreasing Bax protein expression levels, which was shown using western blotting analysis. Histopathological observation also revealed that ginsenoside Rk1 pretreatment significantly reversed APAP-induced necrosis and inflammatory infiltration in liver tissues. Biological indicators of nitrative stress, such as 3-nitrotyrosine, were also inhibited after pretreatment with Rk1 compared with the APAP group.
Conclusion: The results clearly suggest that the underlying molecular mechanisms in the hepatoprotection of ginsenoside Rk1 in APAP-induced hepatotoxicity may be due to its antioxidation, antiapoptosis, anti-inflammation, and antinitrative effects.

1. Introduction

The liver, as an important metabolic organ, is responsible for clearing many poisons and drugs but can also be damaged by these same harmful substances [1]. Recently, acute liver failure has been considered one of the major diseases and has posed growing threats to human health worldwide. It is well accepted that many factors, including infection of the hepatitis virus and exposure to toxins, can lead to acute liver failure [2]. Paracetamol (APAP) is relatively safe and has almost no side effects in the therapeutic dose range and is widely used to treat various painful conditions [3]. However, in the past several decades, clinical data monitoring indicated that an overdose of APAP can cause hepatotoxicity and nephrotoxicity [4]. Widespread use of APAP in hundreds of prescription and over-the-counter drugs has led to the prevalence of APAP-induced hepatotoxicity [5].

Until now, although the exact mechanisms underlying APAP-induced hepatotoxicity remain unclear, growing evidence indicates that multiple mediators of inflammation and oxidative stress contribute to the pathology process of APAP-induced acute

* Corresponding author. College of Chinese Medicinal Materials, Jilin Agricultural University, Changchun 130118, China.
E-mail address: liwei7727@126.com (W. Li).

http://dx.doi.org/10.1016/j.jgr.2017.07.003
p1226-8453 e2093-4947/$ – see front matter

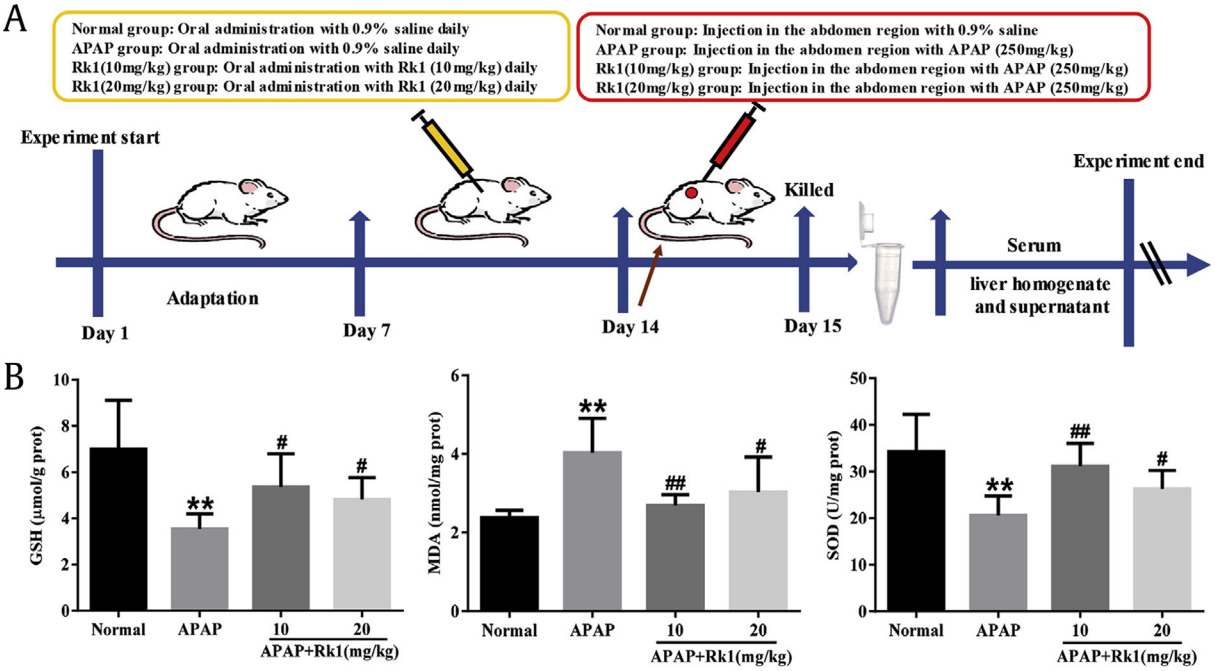

Fig. 1. Pretreatment with Rk1 protected against APAP-induced liver injury. (A) Experimental design of the hepatoprotective effect of Rk1 on APAP-induced liver injury in mice. (B) The levels of GSH, MDA and SOD in liver tissues of mice (B). All data are expressed as the mean ± standard deviation, $n = 8$. $^{**}p < 0.01$ versus normal group; $^{\#}p < 0.05$ versus APAP group; $^{\#\#}p < 0.01$. APAP, paracetamol; GSH, glutathione; MDA, malondialdehyde; prot, protein; SOD, superoxide dismutase.

liver damage [6]. These inflammatory mediators include tumor necrosis factor-α (TNF-α), interleukin-1β (IL-1β), interleukin-10 (IL-10), cyclooxygenase-2 (COX-2), and inducible nitric oxide synthase (iNOS) [7]. *N*-acetyl-*p*-benzoquinone imine (NAPQI), known as a putative reactive metabolite of APAP, can accumulate when APAP concentration is at a high level in the human body and will result in consumption of glutathione (GSH), thus decreasing GSH stores [8]. The excess NAPQI unbound to GSH may undergo a rapid reaction with the mercapto groups of cellular proteins [9]. This process can result in an increase of reactive oxygen species (ROS) and initiates lipid peroxidation (LPO) that eventually results in hepatic destruction, necrosis, or apoptosis [10,11]. The lipid peroxidation products may include malondialdehyde (MDA) and 4-hydroxynonenal (4-HNE) [12,13]. Although many active compounds found in natural medicines have been clinically and experimentally investigated for their ability to protect against APAP-induced hepatotoxicity [14,15], the need for new treatment protocols remains urgent.

The roots of *Panax ginseng* Meyer (ginseng), a traditional Chinese medicine, has been reported to have an adaptogenic effect on endocrine, immune, cardiovascular, and central nervous systems [16,17]. Ginsenosides, considered to be the major active ingredients isolated from the whole ginseng plant, exert numerous pharmacological actions including antidiabetes, antioxidation, anticancer, and anti-inflammation [18,19]. Previous studies have demonstrated that the pharmacological activities of steam-processed ginseng (e.g., red ginseng and black ginseng) are more powerful than unsteamed ginseng (e.g., white ginseng) [20]. Growing evidence has shown that a heating treatment will contribute to extensive conversion of original ginsenosides from unheated ginseng to rare ginsenosides with less polarity, such as ginsenosides 20(R)-Rg3, 20(S)-Rg3, Rg5, Rk1, F4, Rg6, Rs4, and Rs5 [21,22]. Ginsenoside Rk1, a major rare saponin obtained from heat-processed ginseng [23], exerts several biological actions, including antiapoptotic [24], anticancer [25], and antiplatelet aggregation [26]. Although it has been previously reported that fermented ginseng containing a rare ginsenoside (compound K) can alleviate APAP-induced liver injury in a rat model [19], the hepatoprotective effects of ginsenoside Rk1 on APAP-caused hepatotoxicity *in vivo* has not been studied so far. Therefore, the present study was designed to evaluate the effects of ginsenoside Rk1 on APAP-caused liver damage and give insight into its possible mechanisms.

Based on the facts above, we decided to research whether or not ginsenoside Rk1 could exert the potential ameliorative effect on APAP-induced liver hepatotoxicity in a mouse model. More importantly, as far as we know, this is the first time the potential mechanisms underlying such hepatoprotective effects of Rk1 have been uncovered.

2. Materials and methods

2.1. Chemicals and reagents

The ginsenoside Rk1 (purity > 95%) was isolated from black ginseng as described in our previous work [27]. The APAP (>98.0%, UV-VIS, batch no. A7685-100G) was purchased from Sigma–Aldrich (St Louis, MO, USA). The assay kits for alanine aminotransferase (ALT), aspartate aminotransferase (AST), GSH, superoxide dismutase (SOD), and MDA were provided by Nanjing Jiancheng Biological Research Institute (Nanjing, China). Two-site sandwich enzyme-linked immunosorbent assay (ELISA) kits for the detection of mouse TNF-α and IL-1β were purchased from R&D systems (Minneapolis, MN, USA). Hematoxylin–eosin (H&E) and Hoechst 33258 dye kits were obtained from Beyotime Co., Ltd. (Shanghai, China). Two-site immunohistochemical assay kits, SABC-DyLight 488 and SABC-Cy3, and immunofluorescence staining kits were from BOSTER Biological Technology (Wuhan, China). The antibodies, including rabbit monoclonal anti-iNOS, anti-COX-2, anti-Bax, anti-Bcl-2, anti-cytochrome P450 E1 (CPY2E1), anti-4-HNE, and anti-3-nitrotyrosine (3-NT), were provided by BOSTER Biological Technology (Wuhan, China) or Cell Signaling Technology (Danvers, MA, USA). *In situ* Cell Death Detection Kit was provided by Roche Applied Science (No. 11684817910; Roche Applied Science, Penzberg, Germany). All other reagents and chemicals, unless indicated, were obtained from Beijing Chemical Factory (Beijing, China).

2.2. Animals and experimental protocol

Thirty-two male imprinting control region (ICR) mice (8 wk old), weighing 22–25 g, were purchased from Changchun Yisi Experimental Animal Co. Ltd. (Changchun, China). All mice were housed under standard animal holding conditions (12 h light/dark cycle, relative humidity 60 ± 5%, and 25 ± 2°C) for 1 wk to acclimatize to the new conditions before the experiment. All experiments were performed in strict accordance with the Regulations of Experimental Animal Administration from the Ministry of Science and Technology of China. All experimental procedures in this work were approved by the Ethical Committee for Laboratory Animals at Jilin Agricultural University (Permit No.: ECLA-JLAU-16050).

After adaptive breeding for at least 1 wk, the animals were randomly divided into four groups with eight mice per group: normal group; APAP (250 mg/kg) group; APAP+Rk1 (10 mg/kg) group; and APAP+Rk1 (20 mg/kg) group. Ginsenoside Rk1 was prepared by suspending in 0.05% (w/v) sodium carboxymethylcellulose. Ginsenoside Rk1 was gavaged to the mice in treatment groups for 7 consecutive d, mice in the normal and APAP groups were treated with 0.9% saline in the same way. After final administration, mice in the APAP and APAP+Rk1 treatment groups were given a single intraperitoneal injection of APAP with a dose of 250 mg/kg to induce acute liver injury. Meanwhile, mice in the normal group were given 0.9% saline in the same way. The experimental design of the hepatoprotective effect of Rk1 on mice is summarized in Fig. 1A.

All of the mice were fasted for at least 12 h before intraperitoneal injection with APAP and dissection, but they were allowed free access to water. Subsequently, all of the mice were killed by cervical vertebra dislocation at 24 h after the single APAP injection, and their blood

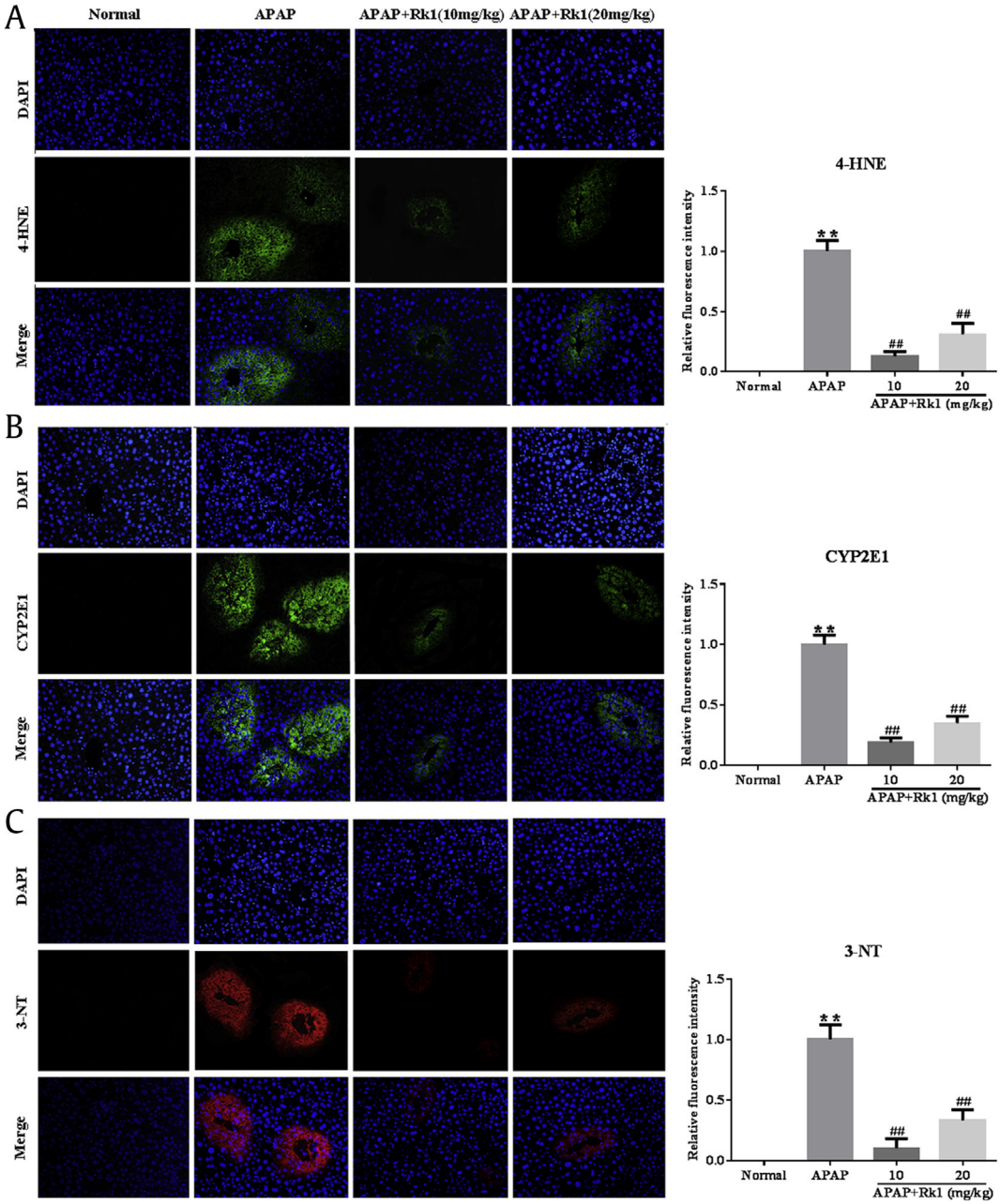

Fig. 2. Pretreatment with Rk1 protected against APAP-induced liver injury. (A) 4-hydroxynonenal (4-HNE), (B) cytochrome P450 E1 (CYP2E1), and (C) 3-nitrotyrosine (3-NT). The expression levels of 4-HNE, CYP2E1 (green) and 3-NT (red) in tissue sections isolated from different groups were assessed by immunofluorescence. Representative immunofluorescence images were taken at 200×. 4′, 6-diamidino-2-phenylindole (DAPI) (blue) was used as a nuclear counterstain. All data are expressed as the mean ± standard deviation, $n = 8$. $^{**}p < 0.01$ versus normal group; $^{\#\#}p < 0.01$ versus APAP group. APAP, paracetamol.

was harvested and stored at −20°C for the determination of two aminotransferases and inflammatory indices. Segregated livers were washed twice with saline, blotted dry on a filter paper, and weighed. At the same time, shape, color, and size of the livers were observed. Liver tissues were dissected quickly and only a small piece was cut off from the same part of the left lobe of each mouse and then fixed in 10% buffered formalin solution (mass/volume) for morphological analysis. The remaining liver samples were thoroughly washed in cold physiological saline and stored at −80°C until required for hepatic homogenate preparation and western blotting analysis.

2.3. Assessment of biochemical parameters

Two important markers of hepatic function, ALT and AST, were determined using commercial kits according to the manufacturer's instructions (Nanjing Jiancheng Bioengineering Research Institute, Nanjing, China).

To assess the hepatic markers of oxidative stress injury, GSH and SOD levels in liver tissues were tested using commercial kits according to the manufacturer's instructions. Liver samples were removed from −80°C and homogenized in ice-cold 0.1M phosphate buffer (pH 7.4), then filtered and centrifuged at 4°C for 10 min. Then the supernatants were analyzed to determine SOD activity and GSH content [28]. Some of the homogenate was used to evaluate LPO by determining thiobarbituric acid reactive substances and was expressed in terms of MDA content, a LPO biomarker.

2.4. Determination of serum TNF-α and IL-1β

After serum samples were obtained, concentrations of TNF-α and IL-1β were determined using ELISA kits according to the protocols provided by the manufacture of R&D systems. In brief, prepared reagents, sample standards, and antibodies labeled with enzymes were added accordingly, then reacted at 37°C for 1 h. After adding stopping solution, the absorbance at 450 nm was measured via an ELISA reader (Bio-Rad, Hercules, CA, USA). To ensure accuracy, all assays were performed in duplicate.

2.5. Histopathological examination

For histopathological examination, the liver samples (n = 8 per group) were fixed over 24 h with 10% buffered formaldehyde before paraffin embedding and sectioning into 5-μm thickness. The liver tissues were routinely stained with H&E dye kits for conventional morphological evaluation using a light microscope (Olympus BX-60, Tokyo, Japan). The degree of hepatocellular necrosis was analyzed by ridit analysis as previously described [29].

2.6. Hoechst 33258 staining

Hoechst 33258 staining was used to observe the nuclear morphological changes of liver tissues, and carried out as previously described with minor modifications according to the manufacturer's protocol [27]. Briefly, the liver tissues were dissected out of mice at the end of the experiment and then fixed in a formalin solution overnight. Three liver tissues were randomly chosen from each group. The 5-μm thickness sections were cut and stained using the Hoechst 33258 solution with 10 μg/mL. After washing with phosphate buffered saline (0.01M, pH 7.4) three times, stained nuclei were visualized under UV excitation and photographed using a fluorescence microscope (Leica TCS SP8, Germany). Image-Pro plus 6.0 (Media Cybernetics, USA) was used to quantify the Hoechst 33258 staining.

2.7. Immunohistochemistry and immunofluorescence analysis

Immunohistochemical staining was performed as previously described with minor modifications [30]. Briefly, 5-μm thick paraffin sections were deparaffinized and rehydrated seriatim in xylene and aqueous alcohol solutions. After antigen retrieval in a citrate buffer solution (0.01M, pH 6.0) for 20 min, the slides were washed with phosphate buffered saline (0.01M, pH 7.4) three times and incubated with 1% bovine serum albumin for 1 h. The blocking serum was tapped off, and the sections were incubated with primary antibodies, including mouse polyclonal anti-iNOS (1:200), anti-COX-2 (1:200), anti-Bax (1:400) and anti-Bcl-2 (1:200), in a humidified chamber at 4°C overnight followed by secondary antibody incubation for 30 min at room temperature. Substrate was added for 30 min followed by DAB staining and hematoxylin counter-staining. The positive staining was determined mainly by a brownish-yellow color in the cytoplasm or nucleus of the cells. An image was taken using light microscopy (Olympus BX-60, Tokyo, Japan), and the cell positive expression intensity was analyzed using Image-Pro Plus 6.0 software.

To evaluate the levels of protein expression of cytochrome P450 E1 (CYP2E1), 4-HNE, and 3-NT in APAP-induced hepatotoxicity, immunofluorescence staining was exerted in liver tissue sections of APAP-induced groups and the normal group as described for immunohistochemistry analysis. In brief, the sections were incubated with the CYP2E1 antibody (1:200), 4-HNE antibody (1:100) and 3-NT antibody (1:200) in a humidified chamber at 4°C overnight. The next day, all slides were marked with a fluorescence secondary antibody for 30 min at room temperature, and then exposed to SABC-DyLight 488 (1:400) or SABC-CY3 (1:100). Nuclear staining in liver tissues was performed using 4, 6 diamidino-2-phenylindole (DAPI) staining. The degrees of immunofluorescence staining in liver tissues were observed using a fluorescence microscope (Leica TCS SP8, Germany), and immunofluorescence intensity was analyzed using Image-Pro Plus 6.0 software.

2.8. Terminal deoxynucleotidyl transferase dUTP nick end labeling assay

For the terminal deoxynucleotidyl transferase dUTP nick end labeling (TUNEL) assay, apoptotic cells in the liver tissues were determined by *in situ* apoptosis detection kits as previously described [31].

Table 1
Effects of Rk1 on body weight, organ indices, and serum biochemical markers in mice

Groups	Dosage (mg/kg)	Body weight (g)		Liver index (mg/g, ×100)	Spleen index (mg/g, ×100)	ALT (U/L)	AST (U/L)
		Initial	Final				
Normal	—	29.74 ± 1.16	33.23 ± 1.16	5.69 ± 0.39	0.46 ± 0.04	23.85 ± 3.86	10.69 ± 4.16
APAP	—	29.97 ± 1.25	27.07 ± 1.18*	6.50 ± 0.52**	0.58 ± 0.06**	114.03 ± 5.90**	64.87 ± 13.18**
APAP + Rk1	10	29.68 ± 1.43	31.29 ± 1.34#	5.70 ± 0.37##	0.47 ± 0.03##	28.32 ± 8.63##	21.73 ± 5.24##
APAP + Rk1	20	29.71 ± 1.49	30.45 ± 1.62	5.89 ± 0.36#	0.49 ± 0.07#	31.80 ± 7.64##	24.05 ± 8.19##

Values represent the mean ± standard deviation, $n = 8$
*$p < 0.05$ versus normal group; **$p < 0.01$; #$p < 0.05$ versus APAP group; ##$p < 0.01$
ALT, alanine aminotransferase, APAP, paracetamol; AST, aspartate aminotransferase

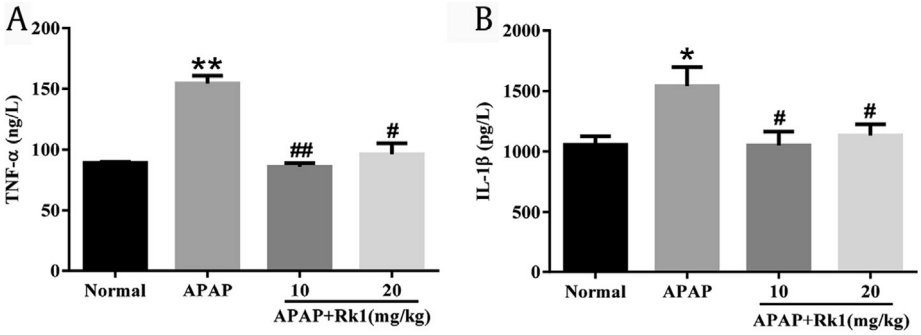

Fig. 3. Pretreatment with Rk1 protected against APAP-induced inflammatory cytokines. The levels of (A) tumor necrosis factor-α (TNF)-α and (B) interleukin-1β (IL)-1β in the serum of mice. All data are expressed as the mean ± standard deviation, $n = 8$. $^{*}p < 0.05$ versus normal group; $^{**}p < 0.01$; $^{\#}p < 0.05$ versus APAP group; $^{\#\#}p < 0.01$. APAP, paracetamol.

Briefly, the proteinase K with 20 μg/mL of distilled water was added to the slides for 10 min at room temperature. The slides were incubated in methanol containing 3% hydrogen peroxide for 20 min and then incubated with an equilibration buffer and terminal deoxynucleotidyl transferase to block endogenous peroxidase. Finally, the sections were incubated with an anti-digoxigenin–peroxidase conjugate. Peroxidase activity of each section was shown using an application of diaminobenzidine. Hematoxylin was used for section counterstaining.

2.9. Western blotting analysis

Western blotting analysis was performed as previously described in our laboratory [18]. Briefly, the liver tissues were homogenized using a Radio-Immunoprecipitation Assay (RIPA) buffer (1:10, m/v). The protein concentrations were measured using a bicinchoninic acid assay (BCA) protein assay kit (Thermo Scientific, Waltham, MA, USA) and normalized to 5 mg/mL. Fifty μg per lane of protein were loaded on 12% sodium dodecyl sulfate–polyacrylamide gel electrophoresis and transferred to polyvinylidene fluoride membrane, and then blocked with 5% skim milk in Tris-buffered saline containing 0.1% Tween-20 for at least 1 h. The membranes were incubated overnight with primary antibodies against Bax (1:2000) and Bcl-2 (1:2000) at 4°C. Then, the membranes were incubated with the secondary antibodies for 1 h at room temperature. Signals were detected using an ECL substrate (Thermo Scientific). Expression in the protein levels were measured with western blotting using Bio-Rad Laboratories-Segrate, Italy (Bio-Rad). The intensity of the bands were quantified by densitometry.

2.10. Statistical analysis

All data are expressed as the means ± standard deviation. The data were analyzed using a two-tailed test or a one-way analysis of variance. GraphPad Prism 6.0 (GraphPad, La Jolla, CA, USA) was used to create the resulting data charts. Ridit analysis, a nonparametric evaluation method, was used for histological examination comparison between groups. Statistical significance was considered to be $p < 0.05$ or $p < 0.01$.

3. Results

3.1. Effects of ginsenoside Rk1 on body weight and organ indices in mice

Generally, the body weight and organ indices are considered to be a putative indicator of health. As shown in Table 1, 24 h after APAP injection, the body weight of mice exposed to APAP 250 mg/kg resulted in notable weight loss compared to mice in the normal group ($p < 0.05$). In addition, the liver and spleen indices were similar in all treated mice; a significant increase was observed in the mice treated with APAP alone ($p < 0.01$). However, in the two treatment groups (10 mg/kg and 20 mg/kg), these changes were significantly reduced ($p < 0.01$, $p < 0.05$).

3.2. Effects of ginsenoside Rk1 on serum biochemical markers

To evaluate whether or not ginsenoside Rk1 preserves liver function, the serum levels of two transaminases (ALT and AST) were determined in all groups 24 h after APAP challenge. As shown in Table 1, the levels of these two transaminases were both dramatically elevated ($p < 0.01$) following a single APAP injection, reflecting a severe liver injury. However, pretreatment with Rk1 for 7 d (10 mg/kg and 20 mg/kg) reversed the increase caused by APAP ($p < 0.01$).

3.3. Effects of ginsenoside Rk1 on oxidative stress markers

As mentioned above, oxidative stress injury was one of the most important mechanisms of APAP-induced hepatotoxicity in a mouse model *in vivo* [32]. In the present study, the results showed that APAP exposure resulted in the depletion of GSH and a dramatic decrease of SOD activity along with an increase of MDA levels in liver tissues, compared to mice in the normal group ($p < 0.01$; Fig. 1B). Interestingly, a significant decrease of MDA levels and restored hepatic SOD activity and GSH content ($p < 0.01$, $p < 0.05$) were observed after pretreatment with ginsenoside Rk1 for 7 d. These data clearly demonstrate that ginsenoside Rk1 alleviated liver oxidative stress injuries. To further confirm whether or not oxidative stress is involved in the development of APAP-induced hepatotoxicity *in vivo*, the degree of lipid peroxidation was determined using 4-HNE staining. After APAP exposure for 24 h, we observed the strong fluorescence intensity of 4-HNE expression in the liver tissues of mice. However, ginsenoside Rk1 pretreatment with two doses (10 mg/kg and 20 mg/kg) for 7 d significantly decreased fluorescence intensity, especially in the low-dose group (Fig. 2A). Interestingly, the location of lipid peroxidation showed high correlations with that of hepatocyte necrosis sites.

Since CYP-mediated bioactivation is considered to play a key role in APAP-induced hepatotoxicity, the protein expression of CYP2E1 in liver tissues was checked after APAP challenge. As expected, APAP challenge after 24 h resulted in overexpression of the CYP2E1 metabolizing enzyme using immunofluorescence analysis. However, treatment with Rk1 decreased the expression of CYP2E1 (Fig. 2B). These results also suggest to some extent that pretreatment of ginsenoside Rk1 attenuates APAP-induced oxidative stress injury.

3.4. Ginsenoside Rk1 ameliorates APAP-induced nitrative stress

To confirm whether or not nitrative stress participates in the pathological process of APAP-induced hepatotoxicity *in vivo*, a nitrative stress marker was confirmed using immunofluorescence

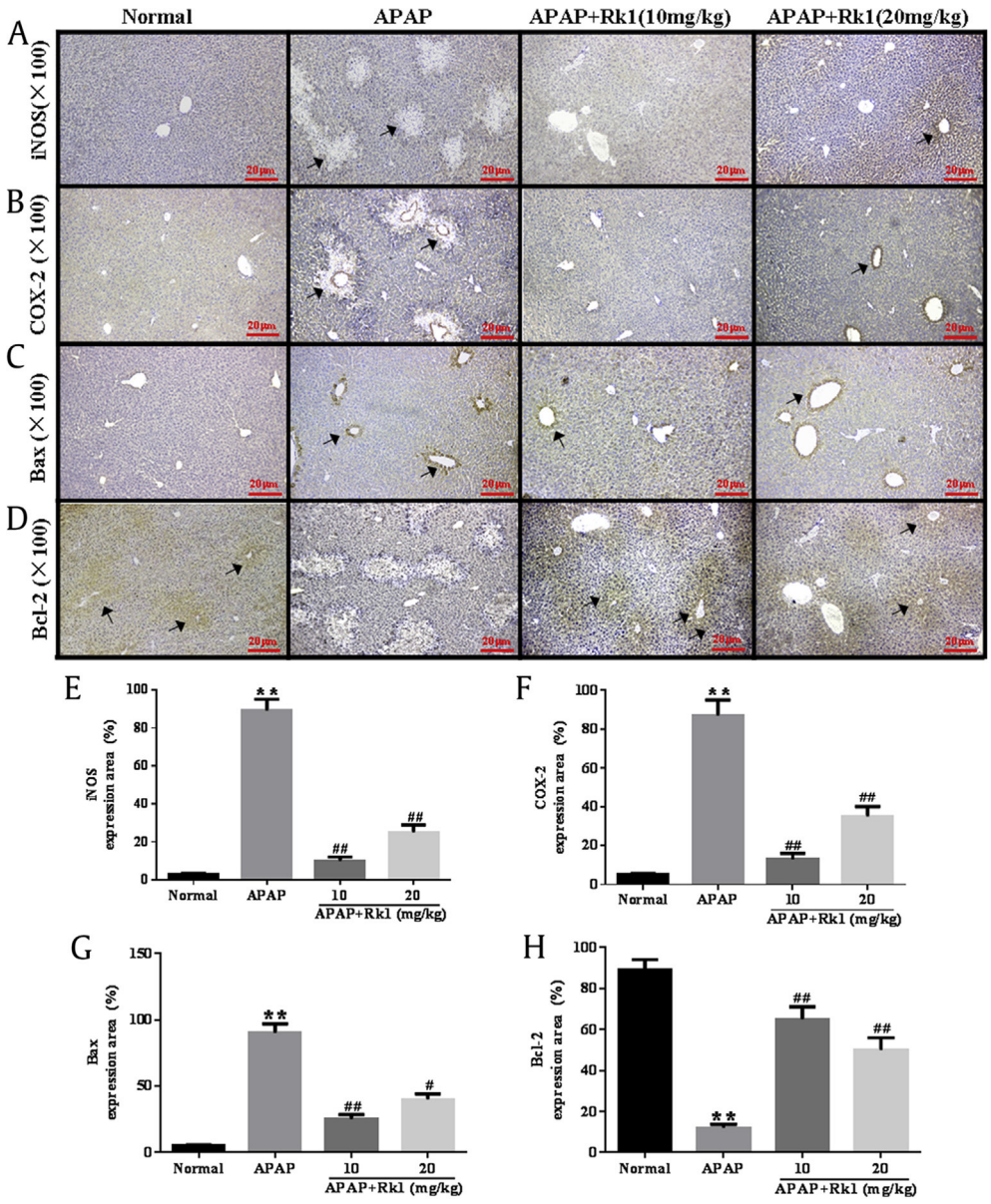

Fig. 4. Pretreatment with Rk1 protected against APAP-induced liver of Rk1 on the expression of: (A, E) nitric oxide synthase (iNOS), (B, F) cyclooxygenase-2 (COX-2), (C, G) Bax, and (D, H) Bcl-2. The protein expression was examined by immunohistochemistry. All data are expressed as the mean ± standard deviation, $n = 8$. $^{**}p < 0.01$ versus normal group; $^{\#}p < 0.05$ versus APAP group; $^{\#\#}p < 0.01$. APAP, paracetamol.

analyses for 3-NT staining. As shown in Fig. 2C, at 24 h after APAP challenge, very strong red fluorescence expression of 3-NT was observed in the central veins of the liver tissues in mice exposed to APAP. In contrast, less 3-NT staining was found in the same area of mice pretreated with ginsenoside Rk1.

3.5. Ginsenoside Rk1 ameliorates APAP-induced liver inflammation

Prevailing evidence indicates that inflammation is involved in the progression of APAP-induced acute liver damage. It has been reported in a previous study that oxidative stress injury is associated with the production of proinflammatory cytokines such as TNF-α, IL-1β, IL-10, and IL-6 [33]. TNF-α, and IL-1β are two major key proinflammatory cytokines involved in the above progression. In our present study, as shown in Fig. 3A and B, APAP injection caused a dramatic increase in serum levels of TNF-α and IL-1β over those in the normal group ($p < 0.01$ and $p < 0.05$, respectively). However, pretreatment with Rk1 significantly inhibited the overproduction of TNF-α and IL-1β ($p < 0.01$ and $p < 0.05$, respectively). Importantly, to further understand the anti-inflammatory effects of ginsenoside Rk1, the expression levels of iNOS and COX-2 in liver tissues were examined using immunohistochemical analyses. As shown in Fig. 4A and B, APAP-treated mice livers stained positive for iNOS and COX-2 in all the observed cytoplasm areas. However, administration of ginsenoside Rk1 with doses of 10 mg/kg and 20 mg/kg resulted in reduced expression of iNOS and COX-2 in liver tissues. The above results indicate that the hepatoprotective effect of ginsenoside Rk1 might also attribute to its anti-inflammatory ability to some extent.

3.6. Ginsenoside Rk1 ameliorates APAP-induced liver histopathological changes

The liver sections of four groups were examined by H&E staining. As shown in Fig. 5A and Table 2, a clear structure of the hepatic lobule, regular hepatic cords with central veins, and a normal cell

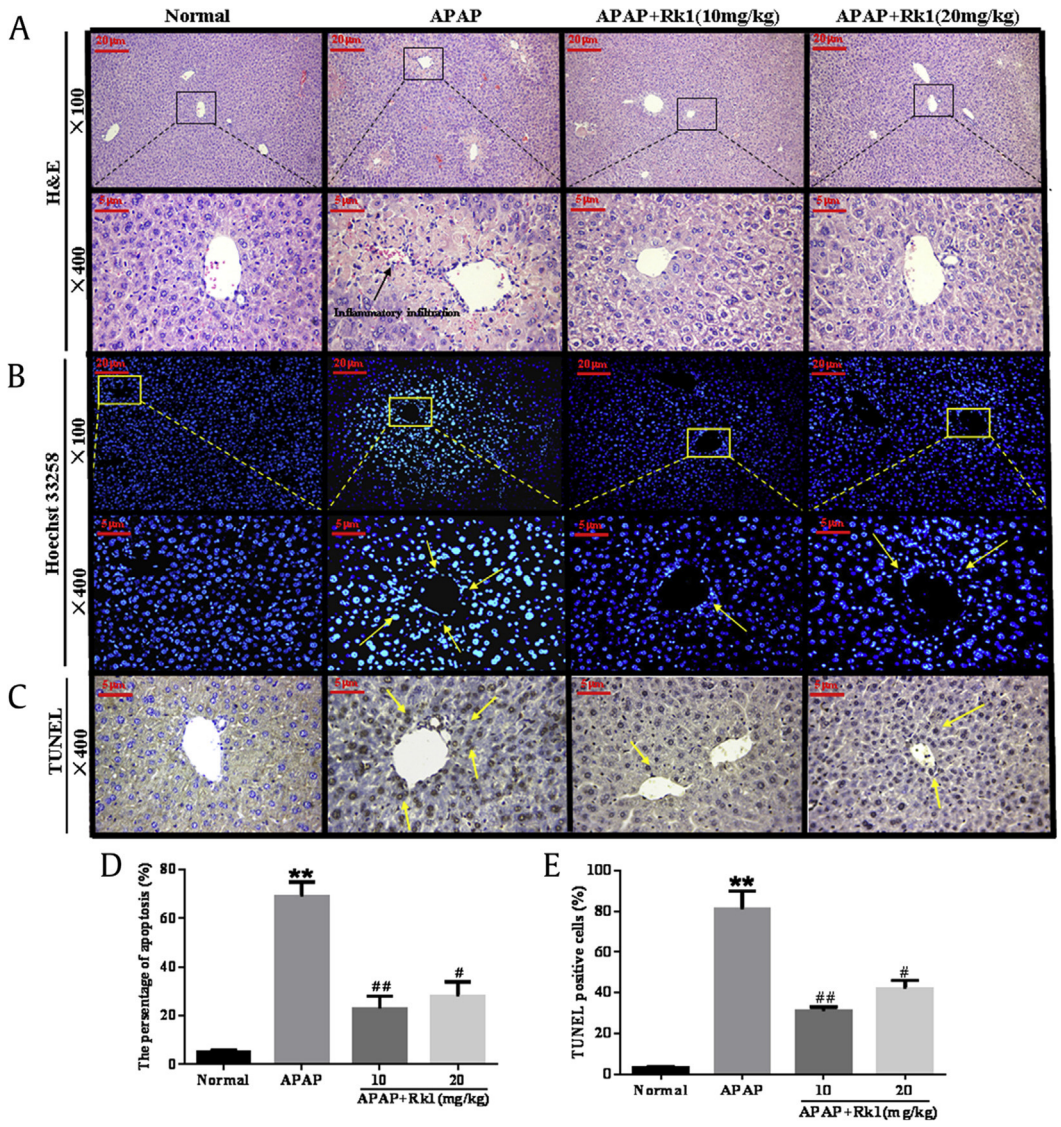

Fig. 5. Histological examination of morphological changes in liver tissues. Liver tissues stained with (A) hematoxylin–eosin (100×, 400×); (B) Hoechst 33258 (100×, 400×) and (D) the percentage of apoptosis; (C) TUNEL (400×) and (E) the presence of TUNEL-positive cells (E). Arrows show necrotic and apoptotic cells. All data are expressed as the mean ± standard deviation, $n = 8$. $^{**}p < 0.01$ versus normal group; $^{\#}p < 0.05$ versus APAP group; $^{\#\#}p < 0.01$. APAP, paracetamol; TUNEL, terminal deoxynucleotidyl transferase dUTP nick end labeling.

nucleus can be observed in hepatic sections of the normal group. However, in the APAP group, typical pathological characteristics, including necrosis, hemorrhage, and inflammatory infiltration, further confirmed the successful establishment of APAP-induced acute liver injury. Pretreatment with Rk1 before APAP exposure noticeably attenuated the inflammation and apoptotic cells. Considering these results, we speculated that Rk1 pretreatment might have an alleviating action on APAP-induced liver injury.

3.7. Ginsenoside Rk1 ameliorates APAP-induced liver cell apoptosis

To determine whether ginsenoside Rk1 pretreatment relieved liver cell apoptosis in APAP-induced acute liver injuries, we used Hoechst 33258 staining to observe the degree of hepatocyte apoptosis. As shown in Fig. 5B and D, the nuclei of the normal group were morphologically intact, neatly arranged with a clear outline, and the chromatin was stained evenly and slightly. However, in the APAP group, distribution over a large area and a high density of blue apoptosis liver cells and small chunks of nuclei were clearly observed, indicating severe apoptosis after APAP challenge. Importantly, after a 7-d continuous pretreatment with ginsenoside Rk1 (10 mg/kg and 20 mg/kg), the apoptosis was alleviated and the liver damage was effectively improved.

To verify the hypothesis that apoptosis may coexist with necrosis in APAP-induced hepatotoxicity, apoptotic liver cells were confirmed and quantified by TUNEL staining. As shown in Fig. 5C and E, almost no apoptotic cells appeared in the liver tissues of the normal group. Compared to the normal group, the quantity of TUNEL-positive cells significantly increased in the APAP-induced group after 24 h. However, ginsenoside Rk1 administration (10 mg/kg and 20 mg/kg) for 7 d remarkably reduced TUNEL-positive cells in liver tissues.

In the present investigation, immunohistochemical and western blotting analyses were used to further determine the impacts of ginsenoside Rk1 on the proapoptotic factor Bax and antiapoptotic factor Bcl-2 in all experimental groups in order to test the extent of apoptosis in liver tissues. As depicted in Fig. 4C and D, Bax-positive expression was unevenly located in the cytoplasm of liver cells. The rate of Bax-positive expression was found to be significantly lower in the Rk1 pretreatment groups than in the APAP group. Bcl-2-positive expression was also observed in liver cell cytoplasm, and

Table 2
Pathological changes in the liver and ridit analysis

Groups	Dosage (mg/kg)	Necrocytosis grade					Score	Ridit analysis
		n	0	1	2	3	4		
Normal	—	8	8	0	0	0	0	0	0.21
APAP	—	7	0	0	2	3	2	21	0.84**
APAP+Rk1	10	8	3	2	2	1	0	9	0.48#
APAP+Rk1	20	8	2	3	2	1	0	10	0.52#

Necrocytosis was classified based on hematoxylin–eosin staining of liver sections. Data were analyzed by ridit analysis. Values represent the mean ± standard deviation

**$p < 0.01$ versus normal group; #$p < 0.05$ versus APAP group

Grading standard: level 0, no necrocytosis, normal liver cells; level 1, liver cells contain necrocytosis of no more than 1/4; level 2, liver cells contain necrocytosis of no more than 1/2; level 3, liver cells contain necrocytosis of no more than 3/4; level 4, liver tissue was almost all necrocytosis. Level 0 calculated 0 marks; Level I calculated 1 mark; Level II calculated 2 marks; Level III calculated 3 marks; Level IV calculated 4 marks. APAP, paracetamol.

there was a significant increase of Bcl-2 expression in the APAP+Rk1 (10 mg/kg) group compared to the APAP group. In addition, western blotting was employed to analyze the proapoptotic factor Bax and anti-apoptotic factor Bcl-2. Pretreatment with ginsenoside Rk1 decreased the protein expression of Bax and the ratio of Bax / Bcl-2, while it increased Bcl-2 protein expression (Fig. 6). These results are almost in line with those from the immunohistochemical analysis.

4. Discussion

APAP is the most widely used antipyretic analgesic and is the most common cause of acute liver failure. When establishing an animal model, APAP is also widely used in the study for evaluating the protective effects of natural medicines and compounds [14]. APAP is the most widely used over-the-counter medication with almost no side effects within the therapeutic dose range. However, long-term or overdose usage of APAP can result in inflammation and necrosis of hepatocytes or even acute liver failure [34]. In 2011, the United States Food and Drug Administration issued a regulation that the content of APAP in prescription drugs should not be > 325 mg per single dose, and limited the maximum daily recommended dose of APAP to < 4.0 g for an adult [35]. The medication guide in Chinese Pharmacopoeia also issued a regulation that the recommended dose of APAP should be not > 2 g per single dose. In clinical practice, the recommended dose is one or two tablets every 4–6 h, but with such a prescription regimen, a patient could easily exceed the recommended maximal daily dose of APAP [36]. Therefore, it is necessary to research new drugs to protect hepatic patients from APAP-induced hepatotoxicity. Currently, APAP is recognized for commonly being used *in vivo* in animal models to result in acute hepatotoxicity to evaluate the hepatoprotective effects of natural medicines [15]. Recent research has identified mice as a more clinically relevant model of APAP toxicity, due to similar susceptibility to and mechanisms of toxicity in mice and human [37]. At present, there has been good progress in the prevention and treatment of APAP-induced liver injuries. The protective mechanisms involved include regulating oxidative stress, an inflammatory reaction, and APAP metabolic excretion [16]. Based on the current understanding, a large number of related target proteins exit in the signal transduction mechanism of APAP hepatotoxicity.

Ginseng, the root of *P. ginseng*, is a famous traditional Chinese medicine widely used in China, Korea, and Japan due to its powerful pharmacological activity. Ginsenosides are divided into two types, including protopanaxadiol-type and protopanaxatriol-type ginsenosides. The protopanaxatriol-type ginsenosides mainly include ginsenoside Rb1, Rb2, Rb3, Rc, and Rd [35]. It has been demonstrated that steamed ginseng exhibits stronger pharmacological activities and therapeutic efficacy than nonsteamed ginseng [38]. The differences among the biological effects can be attributed to significant changes of ginsenosides during the steaming process [39]. Ginsenosides in white ginseng underwent deglycosylation, dehydration, and isomerization to generate many rare ginsenosides during the steaming process [40]. Of these rare ginsenosides, Rk1 and Rg5 were major ones produced from protopanaxadiol-type ginsenosides in the above reaction [41]. As one of the major rare saponins from the heat-processing of ginseng, ginsenoside Rk1 exerts many biological effects, including antiapoptotic, anticancer, and anti-platelet aggregation activities [24–26]. Although fermented ginseng was reported to contain more rare ginsenosides

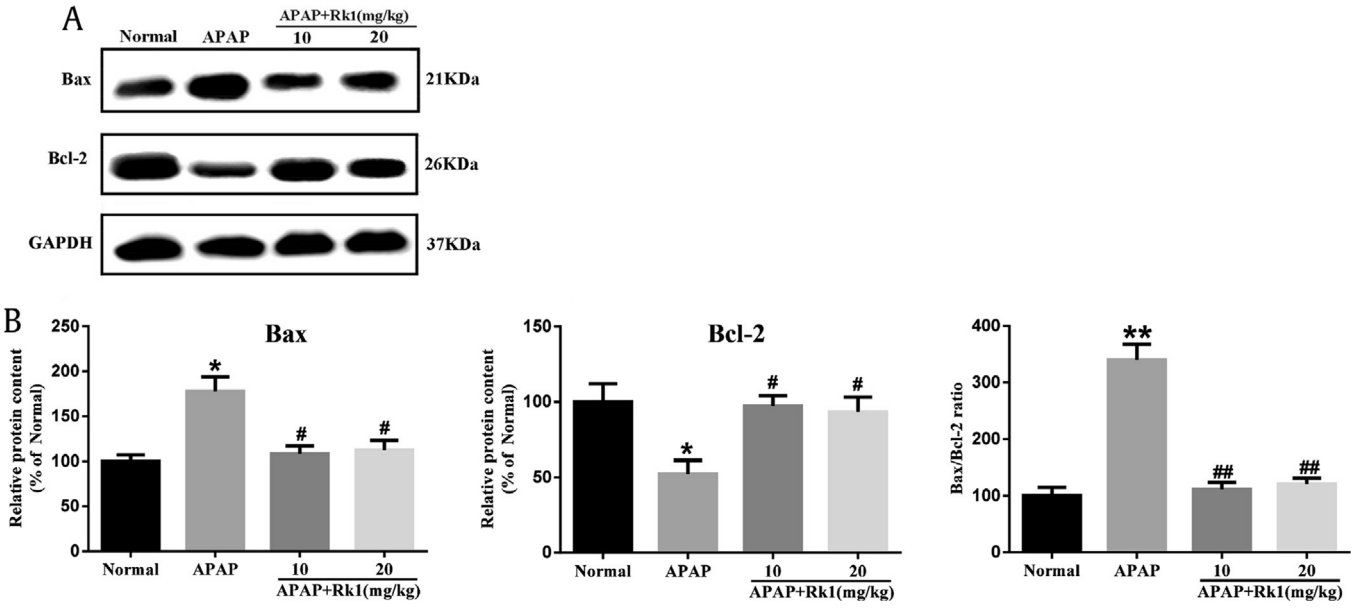

Fig. 6. Protein expression of Bax and Bcl-2. (A) Effects of Rk1 on the protein expression of Bax and Bcl-2. (B) Results quantified from Bax and Bcl-2 band intensities. The protein expression was examined using western blotting analysis in liver tissues. All data are expressed as the mean ± standard deviation, $n = 8$. *$p < 0.05$ versus normal group; **$p < 0.01$; #$p < 0.05$ versus APAP group; ##$p < 0.01$. APAP, paracetamol.

and could alleviate APAP-induced liver injury in a mouse model [42], the exact ameliorative effect and the possible molecular mechanisms of ginsenoside Rk1 on APAP-induced hepatotoxicity was still not clear. Therefore, the aim of our present work was to evaluate the hepatoprotective effects and underlying mechanisms of ginsenoside Rk1 on APAP-intoxicated mice.

In the present study, ginsenoside Rk1 was found to attenuate APAP-induced hepatotoxicity, thus reducing the damage of liver central veins and liver oxidative stress, as well as inhibiting hepatocyte apoptosis and the inflammatory response in an ICR mouse model. Serum ALT and AST are the most sensitive biomarker enzymes used to evaluate drug/chemical-induced acute liver injuries [14]. In our study, 24 h after APAP injection, there was a significant increase in the serum levels of ALT and AST in APAP-injected mice compared with the normal group, suggesting infliction of acute liver damage after APAP exposure. The above results clearly demonstrate that Rk1 inhibited the remarkable increase in serum levels of ALT and AST, indicating significantly protective effects of Rk1 against APAP-induced liver damage. However, this non−dose-dependent effect may be ascribed to the toxicity of saponin ingredients found in high doses of Rk1, which was consistent with previous studies [43].

Oxidative stress, another significant pathogenic factor of APAP-induced hepatotoxicity, has been reported in numerous animal models [44]. It is well accepted that APAP administration is associated with the increasing formation of free radicals, heavy oxidative stress and lipid peroxidation. *In vivo*, APAP is metabolized by cytochrome P450 to toxic NAPQI, which immediately conjugates with GSH [45]. Therefore, overdose of APAP may cause significant GSH depletion in the liver, and result in severe necrosis of liver cells, acute liver failure or even death [46]. The level of MDA is usually considered an important biomarker of oxidative stress and lipid peroxidation injuries [12]. Previous reports have confirmed that elevated MDA levels in liver tissues increases oxidative stress and lipid peroxidation, thus causing liver tissue damage and the collapse of antioxidant defense systems [47]. SOD enzyme, as a member of the enzymatic antioxidant defense system, is able to convert superoxide radicals into molecular oxygen and hydrogen peroxide and thus protect cells from oxidative damage induced by superoxide and hydrogen peroxide radicals [48,49]. In the present investigation, APAP exposure after 24 h significantly increased MDA levels in liver tissues, while pretreatment with a double dose of ginsenoside Rk1 effectively reversed the alterations to a certain degree. Our data showed that the GSH and SOD levels in liver tissues after Rk1 pretreatment significantly increased compared with the APAP group. Therefore, an increase of GSH and SOD and a decreasing level of MDA in liver tissues treated with Rk1 indicate a host-detoxification process of Rk1 in APAP-induced liver injuries. Several reports have demonstrated that the drug-metabolizing enzyme CYP2E1 plays a vital role in APAP-induced hepatotoxicity [50]. In the present investigation, overexpression of CYP2E1 in liver tissues treated with APAP could be reversed after treatment with ginsenoside Rk1. Consistent with the result of MDA, although 4-HNE immunofluorescence staining exhibited high fluorescence intensity in liver tissues after APAP exposure, this process was significantly reversed after administration of ginsenoside Rk1 for 7 consecutive d.

The nitration of tyrosine (i.e., formation of 3-NT), regarded as an important biomarker of peroxynitrite formation, is generally accepted to occur in the liver cells of overdose APAP-challenged mice [51]. A quick interaction between nitric oxide and superoxide is involved in peroxynitrite formation, and peroxynitrile production, increases quickly under the condition of excess APAP exposure [52]. Prior to our work, Jaeschke et al. [53] confirmed that peroxynitrite can cause liver cell necrosis and DNA damage through mitochondrial dysfunction in the pathological process of APAP-induced hepatotoxicity [53]. Importantly, the results from the immunofluorescence analysis clearly showed that overexpression of 3-NT in the liver tissues of APAP-intoxicated mice was in line with the above findings. However, pretreatment with double dose of Rk1 reversed the APAP-mediated increase in 3-NT expression.

Over the past few decades, growing evidence has demonstrated that the inflammation response is also involved in the pathogenesis of hepatotoxicity caused by APAP [7]. Overproduction of inflammatory cytokines can act as a sign of liver damage, while production inhibition of these inflammatory cytokines can help to restore liver function [14]. COX-2 and iNOS are enzymes involved in the inflammatory developing process [54]. Moreover, the overexpression of COX-2 occurred when the liver tissues suffered damage. In addition, proinflammatory cytokines, including TNF-α and IL-1β, are involved in the pathogenesis of hepatotoxicity caused by APAP [7]. Proinflammatory cytokines TNF-α and IL-1β were released from 4 h to 24 h after overdose APAP exposure [14]. Hence, preventing the production of TNF-α or IL-1β may attenuate APAP-induced liver injury. In our study, ginsenoside Rk1 markedly suppressed the release of these inflammatory cytokines caused by APAP exposure, which indicated a potential anti-inflammatory effect of ginsenoside Rk1 in APAP-induced acute hepatotoxicity. Interestingly, the results from the immunohistochemical analysis also revealed that a single APAP injection with 250 mg/kg resulted in the overexpression of iNOS and COX-2 in the liver tissues. Nevertheless, treatment with ginsenoside Rk1 could effectively inhibit the increase of iNOS and COX-2 expression in liver tissues.

Generally, apoptosis is characterized by one of the most fundamental cellular activities to balance the physiological functions of human organisms [55]. Accumulating evidence has indicated that hepatocyte apoptosis is also involved in APAP-induced acute liver injury. Especially, more and more reports have demonstrated apoptosis of hepatocytes after APAP exposure [15]. Two important members of the Bcl-2 family involved in apoptosis are Bax (a pro-apoptotic protein) and Bcl-2 (an anti-apoptotic protein) [56]. Consequently, results from the immunohistochemistry and western blotting analyses showed that the protein expression level of Bax and the ratio of Bax to Bcl-2 were significantly suppressed while the level of Bcl-2 protein expression was relatively increased, clearly indicating that ginsenoside Rk1 exhibits resistance to the effects of apoptosis in APAP-caused hepatotoxicity. In addition, TUNEL and Hoechst 33258 staining were employed to determine the apoptotic hepatocytes in APAP-induced liver injury. The results clearly showed a large area and high density of apoptosis, indicating the apoptosis of liver cells. However, apoptosis in Rk1 groups was alleviated and liver damage was significantly improved. The above data indicate that Rk1 could significantly inhibit hepatocyte apoptosis in APAP-caused hepatotoxicity *in vivo*.

In conclusion, our findings from the present investigation clearly demonstrate that ginsenoside Rk1 can protect against APAP-induced acute liver injuries in mice via the attenuation of oxidative/nitrative stress injuries and the suppression of inflammation and apoptosis. Importantly, these data strongly emphasize that ginsenoside Rk1 seems to be an attractive supplementary drug candidate for the treatment and prevention of liver injury.

Conflicts of interest

The authors declare no conflicts of interest.

Acknowledgments

This work was supported by grants from the National Natural Science Foundation of China (No. 31201331), the Scientific Research Foundation for the Returned Overseas Chinese Scholars (Jilin

Province, 2015), Jilin Science & Technology Development Plan (No. 20160209008YY), and the Program for the Young Top-notch and Innovative Talents of Jilin Agricultural University (2016).

References

[1] Zamora Nava LE, Aguirre Valadez J, Chavez-Tapia NC, Torre A. Acute-on-chronic liver failure: a review. Ther Clin Risk Manag 2014;10:295–303.
[2] Sun H, Chen L, Zhou W, Hu L, Li L, Tu Q, Chang Y, Liu Q, Sun X, Wu M, et al. The protective role of hydrogen-rich saline in experimental liver injury in mice. J Hepatol 2011;54:471–80.
[3] Dargan P, Jones A. Paracetamol: balancing risk against benefit. QJM 2002;95:831–2.
[4] He M, Zhang S, Jiao Y, Lin X, Huang J, Chen C, Chen Z, Huang R. Effects and mechanisms of rifampin on hepatotoxicity of acetaminophen in mice. Food Chem Toxicol 2012;50:3142–9.
[5] Larson AM. Acetaminophen hepatotoxicity. Clin Liver Dis 2007;11:525–48. vi.
[6] Uzkeser M. Protective effect of *Panax ginseng* against N-acetyl-p-aminophenol-induced hepatotoxicity in rats. Afr J Pharm Pharmacol 2012;6:2634–42.
[7] Dragomir AC, Sun R, Mishin V, Hall LB, Laskin JD, Laskin DL. Role of galectin-3 in acetaminophen-induced hepatotoxicity and inflammatory mediator production. Toxicol Sci 2012;127:609–19.
[8] Mitchell JR, Jollow DJ, Potter WZ, Gillette JR, Brodie BB. Acetaminophen-induced hepatic necrosis. IV. Protective role of glutathione. J Pharmacol Exp Ther 1973;187:211–7.
[9] Kon K, Kim JS, Jaeschke H, Lemasters JJ. Mitochondrial permeability transition in acetaminophen-induced necrosis and apoptosis of cultured mouse hepatocytes. Hepatology 2004;40:1170–9.
[10] Hinson JA, Reid AB, McCullough SS, James LP. Acetaminophen-induced hepatotoxicity: role of metabolic activation, reactive oxygen/nitrogen species, and mitochondrial permeability transition. Drug Metab Rev 2004;36:805–22.
[11] Nelson SD. Molecular mechanisms of the hepatotoxicity caused by acetaminophen. Semin Liver Dis 1990;10:267–78.
[12] Lee NH, Seo CS, Lee HY, Jung DY, Lee JK, Lee JA, Song KY, Shin HK, Lee MY, Seo YB, et al. Hepatoprotective and antioxidative activities of cornus officinalis against acetaminophen-induced hepatotoxicity in mice. Evid Based Complement Alternat Med 2012;2012, 804924.
[13] Liu J, Li C, Waalkes MP, Clark J, Myers P, Saavedra JE, Keefer LK. The nitric oxide donor, V-PYRRO/NO, protects against acetaminophen-induced hepatotoxicity in mice. Hepatology 2003;37:324–33.
[14] Zhang Y, Zhang F, Wang K, Liu G, Yang M, Luan Y, Zhao Z. Protective effect of allyl methyl disulfide on acetaminophen-induced hepatotoxicity in mice. Chem Biol Interact 2016;249:71–7.
[15] Wang S, Wang X, Luo F, Tang X, Li K, Hu X, Bai J. Panaxatriol saponin ameliorated liver injury by acetaminophen via restoring thioredoxin-1 and pro-caspase-12. Liver Int 2014;34:1068–73.
[16] Leung KW, Wong AS. Pharmacology of ginsenosides: a literature review. Chin Med 2010;5:20.
[17] Kim SK, Park JH. Trends in ginseng research in 2010. J Ginseng Res 2011;35:389–98.
[18] Li W, Zhang M, Gu J, Meng ZJ, Zhao LC, Zheng YN, Chen L, Yang GL. Hypoglycemic effect of protopanaxadiol-type ginsenosides and compound K on Type 2 diabetes mice induced by high-fat diet combining with streptozotocin via suppression of hepatic gluconeogenesis. Fitoterapia 2012;83:192–8.
[19] Igami K, Shimojo Y, Ito H, Miyazaki T, Kashiwada Y. Hepatoprotective effect of fermented ginseng and its major constituent compound K in a rat model of paracetamol (acetaminophen)-induced liver injury. J Pharm Pharmacol 2015;67:565–72.
[20] Jin Y, Piao J, Lee SM. Evaluating the validity of the Braden scale using longitudinal electronic medical records. Res Nurs Health 2015;38:152–61.
[21] Jiao L, Zhang X, Wang M, Li B, Liu Z, Liu S. Chemical and antihyperglycemic activity changes of ginseng pectin induced by heat processing. Carbohydr Polym 2014;114:567–73.
[22] Park JH, Cha HY, Seo JJ, Hong JT, Han K, Oh KW. Anxiolytic-like effects of ginseng in the elevated plus-maze model: comparison of red ginseng and sun ginseng. Prog Neuropsychopharmacol Biol Psychiatry 2005;29:895–900.
[23] Park IH, Kim NY, Han SB, Kim JM, Kwon SW, Kim HJ, Park MK, Park JH. Three new dammarane glycosides from heat processed ginseng. Arch Pharm Res 2002;25:428–32.
[24] Lee S, Maharjan S, Kim K, Kim NJ, Choi HJ, Kwon YG, Suh YG. Cholesterol-derived novel anti-apoptotic agents on the structural basis of ginsenoside Rk1. Bioorg Med Chem Lett 2010;20:7102–5.
[25] Ko H, Kim YJ, Park JS, Park JH, Yang HO. Autophagy inhibition enhances apoptosis induced by ginsenoside Rk1 in hepatocellular carcinoma cells. Biosci Biotechnol Biochem 2009;73:2183–9.
[26] Ju HK, Lee JG, Park MK, Park SJ, Lee CH, Park JH, Kwon SW. Metabolomic investigation of the anti-platelet aggregation activity of ginsenoside Rk(1) reveals attenuated 12-HETE production. J Proteome Res 2012;11:4939–46.
[27] Li W, Yan MH, Liu Y, Liu Z, Wang Z, Chen C, Zhang J, Sun YS. Ginsenoside Rg5 ameliorates cisplatin-induced nephrotoxicity in mice through inhibition of inflammation, oxidative stress, and apoptosis. Nutrients 2016;8:566.
[28] Li W, Liu Y, Wang Z, Han Y, Tian YH, Zhang GS, Sun YS, Wang YP. Platycodin D isolated from the aerial parts of *Platycodon grandiflorum* protects alcohol-induced liver injury in mice. Food Funct 2015;6:1418–27.
[29] Han Y, Xu Q, Hu JN, Han XY, Li W, Zhao LC. Maltol, a food flavoring agent, attenuates acute alcohol-induced oxidative damage in mice. Nutrients 2015;7:682–96.
[30] Li W, Xu Q, He YF, Liu Y, Yang SB, Wang Z, Zhang J, Zhao LC. Anti-tumor effect of steamed codonopsis lanceolata in H22 tumor-bearing mice and its possible mechanism. Nutrients 2015;7:8294–307.
[31] Xing-yue Xu, Jun-nan Hu, Zhi Liu, Rui Zhang, Yu-fang He, Wei Hou, Zhi-qing Wang, Ge Yang, Wei Li. Saponins (ginsenosides) from the leaves of *Panax quinquefolius* ameliorated acetaminophen-induced hepatotoxicity in mice. J Agric Food Chem 2017;65(18):3684–92.
[32] Nagi MN, Almakki HA, Sayed-Ahmed MM, Al-Bekairi AM. Thymoquinone supplementation reverses acetaminophen-induced oxidative stress, nitric oxide production and energy decline in mice liver. Food Chem Toxicol 2010;48:2361–5.
[33] Barman PK, Mukherjee R, Prusty BK, Suklabaidya S, Senapati S, Ravindran B. Chitohexaose protects against acetaminophen-induced hepatotoxicity in mice. Cell Death Dis 2016;7:e2224.
[34] Jodynis-Liebert J, Matlawska I, Bylka W, Murias M. Protective effect of *Aquilegia vulgaris* (L.) on APAP-induced oxidative stress in rats. J Ethnopharmacol 2005;97:351–8.
[35] Mitka M. FDA asks physicians to stop prescribing high-dose acetaminophen products. JAMA 2014;311:563.
[36] Ghanem CI, Perez MJ, Manautou JE, Mottino AD. Acetaminophen from liver to brain: new insights into drug pharmacological action and toxicity. Pharmacol Res 2016;109:119–31.
[37] McGill MR, Sharpe MR, Williams CD, Taha M, Curry SC, Jaeschke H. The mechanism underlying acetaminophen-induced hepatotoxicity in humans and mice involves mitochondrial damage and nuclear DNA fragmentation. J Clin Invest 2012;122:1574–83.
[38] Jin Y, Kim YJ, Jeon JN, Wang C, Min JW, Noh HY, Yang DC. Effect of white, red and black ginseng on physicochemical properties and ginsenosides. Plant Foods Hum Nutr 2015;70:141–5.
[39] Baek NI, Kim DS, Lee YH, Park JD, Lee CB, Kim SI. Ginsenoside Rh4, a genuine dammarane glycoside from Korean Red Ginseng. Planta Med 1996;62:86–7.
[40] Kim WY, Kim JM, Han SB, Lee SK, Kim ND, Park MK, Kim CK, Park JH. Steaming of ginseng at high temperature enhances biological activity. J Nat Prod 2000;63:1702–4.
[41] Hwang IG, Kim HY, Joung EM, Woo KS, Jeong JH, Yu KW, Lee J, Jeong HS. Changes in ginsenosides and antioxidant activity of Korean ginseng (*Panax ginseng* C.A. Meyer) with heating temperature and pressure. Food Sci Biotechnol 2010;19:941–9.
[42] Hu JN, Liu Z, Wang Z, Li XD, Zhang LX, Li W, Wang YP. Ameliorative effects and possible molecular mechanism of action of black ginseng (*Panax ginseng*) on acetaminophen-mediated liver injury. Molecules 2017;22:664.
[43] Park IH, Piao LZ, Kwon SW, Lee YJ, Cho SY, Park MK, Park JH. Cytotoxic dammarane glycosides from processed ginseng. Chem Pharm Bull (Tokyo) 2002;50:538–40.
[44] Liu LC, Wang CJ, Lee CC, Su SC, Chen HL, Hsu JD, Lee HJ. Aqueous extract of *Hibiscus sabdariffa* L. decelerates acetaminophen-induced acute liver damage by reducing cell death and oxidative stress in mouse experimental models. J Sci Food Agric 2010;90:329–37.
[45] Song Z, McClain CJ, Chen T. S-Adenosylmethionine protects against acetaminophen-induced hepatotoxicity in mice. Pharmacology 2004;71:199–208.
[46] Hsu CC, Lin CC, Liao TS, Yin MC. Protective effect of s-allyl cysteine and s-propyl cysteine on acetaminophen-induced hepatotoxicity in mice. Food Chem Toxicol 2006;44:393–7.
[47] Hsu YW, Tsai CF, Chen WK, Lu FJ. Protective effects of seabuckthorn (*Hippophae rhamnoides* L.) seed oil against carbon tetrachloride-induced hepatotoxicity in mice. Food Chem Toxicol 2009;47:2281–8.
[48] Firuzi O, Miri R, Tavakkoli M, Saso L. Antioxidant therapy: current status and future prospects. Curr Med Chem 2011;18:3871–88.
[49] Weydert CJ, Cullen JJ. Measurement of superoxide dismutase, catalase and glutathione peroxidase in cultured cells and tissue. Nat Protoc 2010;5:51–66.
[50] Hau DK, Gambari R, Wong RS, Yuen MC, Cheng GY, Tong CS, Zhu GY, Leung AK, Lai PB, Lau FY, et al. *Phyllanthus urinaria* extract attenuates acetaminophen induced hepatotoxicity: involvement of cytochrome P450 CYP2E1. Phytomedicine 2009;16:751–60.
[51] Tai M, Zhang J, Song S, Miao R, Liu S, Pang Q, Wu Q, Liu C. Protective effects of luteolin against acetaminophen-induced acute liver failure in mouse. Int Immunopharmacol 2015;27:164–70.
[52] Saito C, Lemasters JJ, Jaeschke H. c-Jun N-terminal kinase modulates oxidant stress and peroxynitrite formation independent of inducible nitric oxide synthase in acetaminophen hepatotoxicity. Toxicol Appl Pharmacol 2010;246:8–17.
[53] Jaeschke H, Williams CD, McGill MR, Xie Y, Ramachandran A. Models of drug-induced liver injury for evaluation of phytotherapeutics and other natural products. Food Chem Toxicol 2013;55:279–89.
[54] Chung WY, Park JH, Kim MJ, Kim HO, Hwang JK, Lee SK, Park KK. Xanthorrhizol inhibits 12-O-tetradecanoylphorbol-13-acetate-induced acute inflammation and two-stage mouse skin carcinogenesis by blocking the expression of ornithine decarboxylase, cyclooxygenase-2 and inducible nitric oxide synthase through mitogen-activated protein kinases and/or the nuclear factor-kappa B. Carcinogenesis 2007;28:1224–31.
[55] Hsu YL, Kuo PL, Liu CF, Lin CC. Acacetin-induced cell cycle arrest and apoptosis in human non-small cell lung cancer A549 cells. Cancer Lett 2004;212:53–60.
[56] Oz HS, Chen TS. Green-tea polyphenols downregulate cyclooxygenase and Bcl-2 activity in acetaminophen-induced hepatotoxicity. Dig Dis Sci 2008;53:2980–8.